The Astrophysical Journal Letters, 730:L19 (5pp), 2011 April 1 doi:10.1088/2041-8205/730/2/L19

ON THE EVOLUTION OF THE MOLECULAR GAS FRACTION OF STAR-FORMING GALAXIES

James E. Geach[1], Ian Smail[2], Sean M. Moran[3], Lauren A. MacArthur[4,5], Claudia del P. Lagos[2], and Alastair C. Edge[2]
[1] Department of Physics, McGill University, 3600 Rue University, Montréal, QC H3A 2T8, Canada; jimgeach@physics.mcgill.ca
[2] Institute for Computational Cosmology, Durham University, South Road, Durham, DH1 3LE, UK
[3] Department of Physics and Astronomy, Johns Hopkins University, Baltimore, MD 21218, USA
[4] Herzberg Institute of Astrophysics, National Research Council of Canada, 5071 West Saanich Road, Victoria, BC V8X 4M6, Canada
[5] Department of Physics & Astronomy, University of Victoria, Victoria, BC V8P 1A1, Canada
Received 2011 January 16; accepted 2011 February 16; published 2011 March 4

ABSTRACT

We present IRAM Plateau de Bure interferometric detections of CO ($J = 1 \rightarrow 0$) emission from a 24 μm-selected sample of star-forming galaxies at $z = 0.4$. The galaxies have polycyclic aromatic hydrocarbon 7.7 μm-derived star formation rates of SFR ∼30–60 $M_\odot$ yr^{-1} and stellar masses $M_\star \sim 10^{11}\ M_\odot$. The CO ($J = 1 \rightarrow 0$) luminosities of the galaxies imply that the disks still contain a large reservoir of molecular gas, contributing ∼20% of the baryonic mass, but have star formation "efficiencies" similar to local quiescent disks and gas-dominated disks at $z \sim 1.5$–2. We reveal evidence that the average molecular gas fraction has undergone strong evolution since $z \sim 2$, with $f_{\rm gas} \propto (1+z)^{-2\pm0.5}$. The evolution of $f_{\rm gas}$ encodes fundamental information about the relative depletion/replenishment of molecular fuel in galaxies and is expected to be a strong function of halo mass. We show that the latest predictions for the evolution of the molecular gas fraction in semi-analytic models of galaxy formation within a ΛCDM universe are supported by these new observations.

Key words: cosmology: observations – galaxies: evolution

Online-only material: color figures

1. INTRODUCTION

Molecular hydrogen is arguably the most important component of the interstellar medium (ISM) in high-redshift galaxies, since it is the phase necessary for, and immediately preceding, star formation. However, observing cool ($\lesssim$50 K) molecular hydrogen is difficult; the molecule has no permanent electric dipole and so one must rely on tracer molecular emission (the most common being rovibrational emission from the ^{12}CO isotopomer, hereafter "CO").

Unfortunately, uncertainty of the precise calibration of CO luminosity to total gas mass in both low- and high-z galaxies has made interpretation of results challenging; even in the local universe there is seen to be metallicity and luminosity dependence on the conversion (Boissier et al. 2003; Blitz et al. 2007; Komugi et al. 2010). Furthermore, although the bulk of the molecular gas in star-forming disks is contained in virialized clouds, it is clear that the most luminous galaxies—mostly mergers—have molecular gas distributions and star formation modes dramatically different to quiescent disks; they require an alternative molecular mass calibration related to the physical conditions of their interstellar media (Solomon et al. 1997). The importance of understanding how the thermodynamic state of the gas affects the calibration also remains controversial (high-z observations typically target $J_{\rm upper} > 1$, requiring some correction to $J = (1 \rightarrow 0)$) based on the excitation of the gas; although see Ivison et al. (2010) and Harris et al. (2010).

The majority of molecular gas studies at high-z have, necessarily, focused on the most active systems (generally submillimeter-selected galaxies and quasars), and so comparatively little is known about the evolution of the molecular gas properties of the more common, but less active population. Nevertheless, recent studies have started to make progress in expanding the parameter space of CO observations at high-z, and several studies have detected CO emission from "normal" disks at $z = 1$–2 (Daddi et al. 2008; 2010; Tacconi et al. 2010). The striking result is that the efficiency of star formation in these distant galaxies is claimed to be similar to that seen in local "quiescent" disks (Dannerbauer et al. 2009; Daddi et al. 2010), with enhanced star formation rates (SFRs) driven simply by larger gas reservoirs, drained by star formation (and feedback) on Gyr timescales. This hints that a secular mode of star formation might be ubiquitous in $L^\star$ disks independent of cosmic epoch (but see the higher-z results of Coppin et al. 2007 and Riechers et al. 2010).

The aim of this Letter is to further expand the parameter space of molecular gas studies in normal galaxies, building on our observations of luminous infrared galaxies (LIRGs) at $z = 0.4$ (Geach et al. 2009a, hereafter G09). We present new IRAM Plateau de Bure interferometric (PdBI) observations of a sample of 24 μm-selected galaxies in the outskirts of the rich cluster Cl 0024+16 at $z = 0.395$. These galaxies bridge the gap between quiescent, local spirals and luminous, high-redshift starbursts and disks. Throughout we adopt a $\Omega_{\rm m} = 0.3$, $\Omega_\Lambda = 0.7$, and $H_0 = 70$ km s^{-1} Mpc^{-1} cosmology.

2. OBSERVATIONS AND DATA REDUCTION

Our sample consists of five *Spitzer* MIPS 24 μm detected LIRG-class galaxies in the outskirts of the rich cluster Cl 0024+16 ($z = 0.395$; see Geach et al. 2006). We obtained mid-infrared spectroscopy with the *Spitzer* Infrared Spectrograph to confirm the presence of aromatic features, a clear indication of star formation (rather than infrared emission dominated by an active galactic nucleus; Geach et al. 2009b). Combined with the two galaxies observed with IRAM PdBI in G09, this represents an effort to obtain CO detections or limits for *all* the galaxies where we have detected significant emission from the polycyclic aromatic hydrocarbon 7.7 μm band. The line luminosities imply SFRs of ∼30–60 $M_\odot$ yr^{-1}, thus allowing us to link molecular gas with moderate levels of dusty star formation in the galaxies.

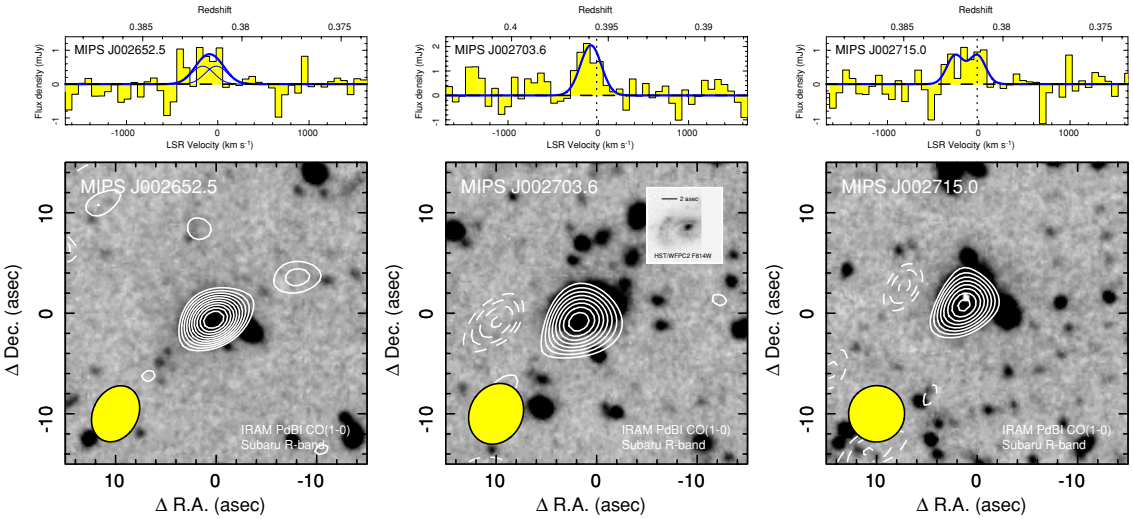

Figure 1. Velocity integrated, clean CO ($J = 1 \rightarrow 0$) line emission maps (at levels of $\geqslant 2 \times$ rms in steps of 0.5) overlaid on $30'' \times 30''$ Subaru SuprimeCam *R*-band images (including a $5'' \times 5''$ *HST*/WFPC2 inset for MIPS J002703.6). The ellipse indicates the beam size and shape. Top: 3 mm spectra extracted from the peak of the integrated line emission maps fit with either a single or double Gaussian (where doubles have a fixed amplitude and width for each peak).

(A color version of this figure is available in the online journal.)

In this Letter, we present the results in the context of the broader star-forming population at $z = 0.4$, rather than focusing on potential environmental effects in the cluster. We believe this is a valid approach, since these galaxies are expected to be randomly accreted onto the cluster from the surrounding field, and the galaxies are seen at a stage where strong environmental effects associated with clusters (specifically ram-pressure stripping and harassment) are yet to have an effect (Treu et al. 2003; Moran et al. 2007). They lie at clustocentric radii of 1.8–4.6 Mpc ($\sim$1–3 $\times$ the virial radius of Cl 0024+16). Intrinsically, they are likely to be representative of disk galaxies of equivalent mass sampled from a random field and can be compared to galaxies with similar properties at low and high redshift, i.e., normal star-forming disks.

The new IRAM observations were conducted over 2009 June–October in configuration "D," using five antennae, and we adopted the same strategy as in G09. Sensitivities ranged between 0.51 and 1.17 mJy (median average for 10 MHz wide channels and two polarizations), and the on-source exposure times ranged between 6.4 and 12.8 hr. We targeted the CO ($J = 1 \rightarrow 0$) 115.27 GHz rotational transition at $\nu_{\rm obs} \simeq 82.63$ GHz in five sources. The 3 mm receiver was tuned to the frequency of the redshifted CO ($J = 1 \rightarrow 0$) line at the systemic redshift of each galaxy derived from optical spectroscopy (Czoske et al. 2001; Moran et al. 2007). As in G09, the correlator was set up with 2.5 MHz spacing (2×64 channels, 320 MHz bandwidth). The phase and flux calibrators were the sources 3C454.3, 0119+115, and 0007+171. The observing conditions were good or excellent in terms of atmospheric phase stability; however, any anomalous and high phase-noise visibilities were flagged in the calibration stage. Data were calibrated, mapped, and analyzed using GILDAS (Guilloteau & Lucas 2000).

3. RESULTS

3.1. Plateau de Bure CO Detections

We detect CO ($J = 1 \rightarrow 0$) emission in three galaxies ($>4\sigma$ detections within $2''$ of the phase tracking center, significances determined from the integrated line flux). Velocity-integrated maps and millimeter spectra are shown in Figure 1. Total fluxes are evaluated from single or double Gaussian fits to the spectra depending on whether the profiles are very broad and have hints that they are double peaked. The line luminosities are in the range $L'_{\rm CO} = (0.26\text{–}0.64) \times 10^{10}$ K km s^{-1} pc^2 (Table 1). Uncertainties on the luminosities are estimated by re-evaluating the Gaussian fits after artificially adding noise to each channel based on the observed rms fluctuations in each data cube. Upper 3σ limits on $L'_{\rm CO}$ for the two non-detections are based on the rms noise in the observations of each source (note that the two non-detections are also the two galaxies with the lowest SFRs in the sample). The luminosities and line widths are listed in Table 1; we also list the properties of the two galaxies from G09 which are included in the following analysis.

The spectra of MIPS J002652.5 and MIPS J002715.0, like MIPS J002721.0 (G09), exhibit broad CO ($J = 1 \rightarrow 0$) emission and can be well fit by double Gaussian profiles. None of the new sample show obvious signs of major mergers or strong tidal interaction in the deep optical imaging (Figure 1), and so we conclude that we are most likely observing CO ($J = 1 \rightarrow 0$) emission tracing molecular gas distributed over rotationally supported disks.

3.2. Physical Properties of the Galaxies

Stellar masses for all the galaxies were determined by fitting the galaxy spectral energy distribution (SED) constructed from *BVRIJK* imaging (Moran et al. 2007) to a large suite of model SEDs using the KCORRECT software, v4.2 (Blanton & Roweis 2007). Utilizing the known spectroscopic redshifts, KCORRECT finds the best non-negative combination of the template spectra to fit the galaxy SED in its rest frame, including a reddening law, with best-fit values covering a range $A_V = 0.8\text{–}2.3$ mag. Stellar masses are then calculated from the luminosity and mass-to-light ratio of the best-fitting model in the rest-frame *K* band, $\Upsilon_\star = M_\odot / L^K_\odot$. The fits had an average mass-to-light ratio of $\langle \Upsilon_\star \rangle = 0.36$ (range 0.24–0.52) and inferred stellar masses ranging over $M_\star \sim (0.5\text{–}1) \times 10^{11}\, M_\odot$ (Table 1).

In G09, we adopted a conservative "ULIRG" conversion of $\alpha = 0.8\ M_\odot\,(\mathrm{K\ km\ s^{-1}\ pc^2})^{-1}$ for gas mass, where $M(\mathrm{H_2 + He}) = \alpha L_\odot$ (we omit the units of α for clarity in the following). However, there are hints that a Galactic scaling

Table 1
Properties of the Galaxy Sample

Target	α_{J2000} (h m s)	δ_{J2000} (° ′ ″)	$z_{[O\,II]}$	L_{FIR} ($10^{11} L_\odot$)	SFR ($M_\odot$ yr^{-1})	$V_{FWHM}^{CO(1-0)}$ (km s^{-1})	$L'_{CO(1-0)}$ (10^{10} K km s^{-1} pc^2)	$M(H_2+He)$[a] ($10^{10}\,M_\odot$)	$M_\star$[b] ($10^{11}\,M_\odot$)	f_{gas}
MIPS J002652.5	00 26 52.5	+17 13 59.9	0.3799	3.5 ± 0.5	62 ± 19	140 ± 10	0.64 ± 0.05	2.9 ± 0.2	0.95	0.23 ± 0.02
MIPS J002703.6	00 27 03.6	+17 11 27.9	0.3956	2.3 ± 0.3	42 ± 12	250 ± 30	0.43 ± 0.06	2.0 ± 0.3	0.87	0.19 ± 0.03
MIPS J002715.0	00 27 15.0	+17 12 45.6	0.3813	1.9 ± 0.3	35 ± 11	340 ± 40	0.26 ± 0.03	1.2 ± 0.3	1.10	0.10 ± 0.03
MIPS J002609.1	00 26 09.1	+17 15 11.5	0.3940	1.5 ± 0.3	28 ± 9	···	<0.39	<1.8	0.41	<0.30
MIPS J002606.1	00 26 06.1	+17 04 16.4	0.3904	1.9 ± 0.3	34 ± 10	···	<0.25	<1.1	0.49	<0.19
MIPS J002621.7[c]	00 26 21.7	+17 19 26.4	0.3803	3.1 ± 0.2	56 ± 16	140 ± 10	0.68 ± 0.06	3.1 ± 0.3	1.12	0.22 ± 0.02
MIPS J002721.0[c]	00 27 21.1	+16 59 49.9	0.3964	3.2 ± 0.2	59 ± 16	160 ± 30	1.14 ± 0.11	5.2 ± 0.5	0.98	0.34 ± 0.04

Notes.
[a] Assuming a CO luminosity to total gas mass conversion factor of $\alpha = 4.6\,M_\odot\,(\mathrm{K\,km\,s^{-1}\,pc^2})^{-1}$ that includes helium.
[b] Uncertainties ∼0.02 dex based on refitting spectral templates 1000 times with random perturbation within 1σ photometric uncertainties.
[c] Geach et al. (2009a).

is more appropriate for these galaxies. The first point to note is the similarity between the so-called star formation efficiencies, measured by L'_{CO}/L_{IR}, compared to local quiescent disks. The disks in this sample have a mean $\langle L_{IR}/L'_{CO}\rangle = 51$ (range 28–73), similar to that of local spirals, but lower than that of ULIRGs, which tend to have $L_{IR}/L'_{CO} \gtrsim 100$ (Solomon et al. 1997). Daddi et al. (2010) and Tacconi et al. (2010) report similar "secular" properties for $z > 1$ disks, although note that these high-z observations measure $J_{up} > 1$ transitions, and so require an additional uncertain correction to estimate gas mass. It is claimed that the efficiency of star formation remains relatively constant in typical disks at all epochs (although, as a concept, star formation "efficiency" only makes sense if all of the molecular gas has an equal probability of undergoing star formation).

Although the CO (and mid-infrared) emission is unresolved, we can evaluate how appropriate $\alpha = 0.8$ is based on the offset from the Kennicutt–Schmidt (K-S) law ($\Sigma_{SFR} \propto \Sigma_{gas}^{1.4}$; Kennicutt 1998), assuming both gas and star formation trace the stellar emission. Inclination and effective radii of the disks are estimated by fitting a two-dimensional model following a Sérsic profile to a Canada–France–Hawaii Telescope (CFHT) R-band image (Czoske et al. 2001), using GALFIT v3.0.2 (Peng et al. 2010). GALFIT was run on postage stamps of $20'' \times 20''$, simultaneously fitting models to the main galaxy and any bright companions in the field. GALFIT produces estimates of the galaxy axial ratio and size that accounts for the seeing of the ground based image, by convolving with a point-spread function that we have extracted from stars in the CFHT image. The effective radii of the disks range between 0.″9 and 1.″5 (4.8–8.1 kpc), with a mean of 1″ (5.4 kpc), and typical uncertainties of 0.″02. We take the effective radii as the size of the disks and find a mean $\langle\alpha_{K\text{-}S}\rangle \sim 4.2$, in line with a Galactic conversion. Note that this should be taken only as a guide for choosing between a Galactic and ULIRG-like conversion, $\alpha_{K\text{-}S}$ should not be applied as the actual calibration: it is particularly sensitive to the assumed spatial distribution of the gas and star formation, such that a larger assumed radius would result in a larger $\alpha_{K\text{-}S}$ and vice versa (with $r \lesssim 1$ kpc required for $\alpha_{K\text{-}S} \sim 0.8$).

MIPS J002703.6 is partially covered by one of the sparse *Hubble Space Telescope* (*HST*)/WFPC2 (F814W) images taken of Cl 0024+16 (Treu et al. 2003), revealing finer detail of the optical morphology (Figure 1). The galaxy has been typed as an early-type spiral (Treu et al. 2003) and has clear spiral structure with several bright knots of emission in the northern arm (presumably star-forming regions) and a potential bar. We have run GALFIT on the *HST*/WFPC2 image, where the best two-dimensional fit is a two-component Sérsic bulge and exponential disk, where the bulge and disk have effective radii of 0.″15 (0.8 kpc) and 1.″05 (5.6 kpc), respectively (consistent with the value derived from the ground-based imaging), and the bulge-to-total light ratio is $B/T = 0.031$.

Based on this evidence, we now assume a Galactic conversion of $\alpha = 4.6$ to estimate the gas masses, which implies molecular gas masses of $M(H_2 + He) = (1.2\text{–}2.9) \times 10^{10}\,M_\odot$. What is the gas contribution to the total baryonic mass of these galaxies? With our choice of α, the resulting gas fractions, $f_{gas} = M_{gas}/(M_{gas} + M_\star)$, are in the range 0.10–0.34, with a mean of $\langle f_{gas}\rangle = 0.21 \pm 0.03$. We can conclude that these are actively star-forming galaxies with large gas reservoirs, but the disks are dominated by stellar mass. This is markedly different to the recently discovered $z \sim 1$–2 gas-rich disks of Daddi et al. (2010) and Tacconi et al. (2010), which are generally more active galaxies, with comparable stellar masses and higher gas fractions $f_{gas} \gtrsim 40\%$.

4. INTERPRETATION

Figure 2 shows the observed f_{gas} in $M_\star \geqslant 10^{10}\,M_\odot$ galaxies at $z = 0$ (Leroy et al. 2008), $z = 0.4$ (this work), and $z = 1.5$–2 (Daddi et al. 2010; Tacconi et al. 2010) showing the clear decline in $\langle f_{gas}\rangle$ in the 10 Gyr since $z \sim 2$. As a guide, we cast the evolution of f_{gas} relative to the cosmological abundance of baryons in stars and molecular gas at $z = 0$: $\Omega_{H_2}/(\Omega_{H_2} + \Omega_\star) = 0.078^{+0.160}_{-0.039}$ from the "baryon census" of Fukugita et al. (1998). At $z = 0$, the observed f_{gas} in star-forming disks is close to that inferred from the total relative abundance of molecular gas and stars in the universe, but at $z \sim 2$ it was a factor ∼5–10 larger than the local value.[6] The decline in molecular gas fraction in the stellar mass limited sample is broadly characterized by $f_{gas} \propto (1+z)^\gamma$, with $\gamma \sim 1.5$–2.5, shallower than the rate of decline of the average specific SFR in galaxies over the same epoch, which falls off more like $(1+z)^4$ (e.g., Karim et al. 2010). This is expected, since molecular reservoirs can be replenished with fresh material via cooling; thus, it is the relative evolution of the cooling rate and SFR that shape the evolution of f_{gas}.

[6] The similarity of the average galaxy gas fraction and the cosmic abundance at $z = 0$ is perhaps coincidental, since $\Omega_\star$ is integrated over the luminosity functions of all bulges, disks, and irregulars, whereas Ω_{H_2} is inferred from a relatively limited local CO survey. However, it could be a convenient datum for comparisons of f_{gas}.

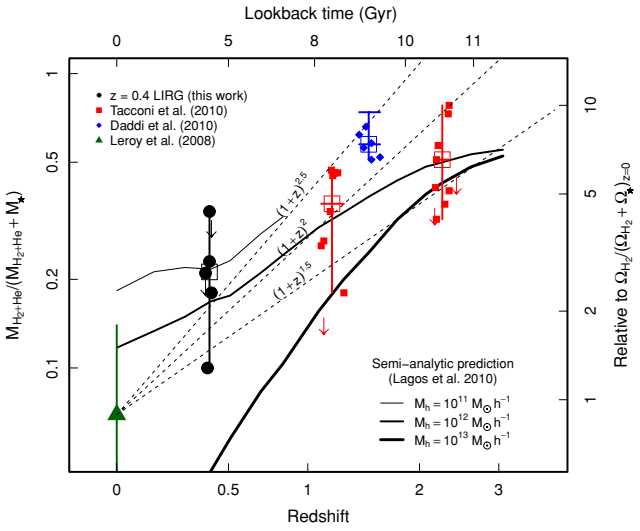

Figure 2. Evolution of the molecular gas fraction in $M_\star > 10^{10}\,M_\odot$ galaxies, showing decline in $f_{\rm gas}$ over cosmic time following $(1+z)^{\sim 2\pm 0.5}$. We compare our $z = 0.4$ results with the high-z disks of Daddi et al. (2010) and Tacconi et al. (2010), and the $z \sim 0$ sample of Leroy et al. (2008). Large open symbols show the average of each sample, with error bars indicating the range. The upper bar of the Daddi et al. sample shows the effect of assuming $\alpha = 4.6$. All stellar mass estimates assume a Chabrier initial mass function (we have applied a factor 1.25 to the Leroy et al. data). We also show the evolution of $f_{\rm gas}$ in galaxies with $M_\star \geqslant 10^{10}\,M_\odot$ in different halos from the latest semi-analytic models (Lagos et al. 2010).

(A color version of this figure is available in the online journal.)

Recent semi-analytic prescriptions for galaxy formation make predictions for the evolution of the molecular ISM. In Figure 2, we show the average $H_2 + He$ fraction in $M_\star \geqslant 10^{10}\,M_\odot$ galaxies selected in halos of various mass from the GALFORM model (galaxies populated within the Millennium Simulation ΛCDM framework). This latest model (Lagos et al. 2010) implements an empirically based star formation law (Blitz & Rosolowsky 2006) to estimate the molecular gas mass. The model predicts that (at $z < 3$), $f_{\rm gas}$ is on average lower, and its evolution stronger in more massive halos. In the mass regime pertinent to our observed sample, $10^{12}\,M_\odot$, the model tracks are well-matched to the observations over $0 < z < 2$. The results are broadly consistent with other models. For example, in smoothed particle hydrodynamic simulations, Kereš et al. (2005) predict that the average accretion rate of gas onto galaxies within halos of $M_{\rm vir} = 10^{12}\,M_\odot$ decreases from $\dot{M}_{\rm cold} \sim 20\,M_\odot\ {\rm yr}^{-1}$ at $z = 2$ to $\dot{M}_{\rm cold} \sim 3\,M_\odot\ {\rm yr}^{-1}$ at $z = 0.4$. The observed evolution is also consistent with the predicted cosmological evolution of the accretion rate at fixed halo mass in other models (see Dutton et al. 2010).

The evolution of $f_{\rm gas}$ is expected to be strongly dependent on galaxy mass, since the evolution of the global average SFR appears to be halo mass dependent, as does the expected evolution of the gas accretion rate. Cooling and star formation are the key drivers of the molecular gas fraction; but it is also sensitive to the merger rate (which can deliver molecular material, trigger star formation, and reconfigure the baryonic content), feedback (heating or ejection of cold gas and H_2 dissociation), environmental effects (e.g., ram-pressure stripping), and growth in size of galaxy disks. The latter has an important effect since it (on average) reduces the disk hydrostatic pressure ($\propto r^2$) and therefore the efficiency of H_2 formation (reflected in the H_2/H I ratio; Elmegreen 1993; Wong & Blitz 2002), as can the metallicity and strength of the interstellar UV radiation field.

Selection effects will affect Figure 2 severely, and we should discuss how these might affect our interpretation. Sensitivity limits do not allow us to detect galaxies with very low gas fractions at high-z, and in low-z surveys the very gas rich systems appear to be rare. Here we have attempted to compare similar galaxies across a range of epochs, but the current sample sizes are small, and inhomogeneously selected; any conclusions we draw from Figure 2 should be treated as indicative for future surveys that can more precisely control selection and have the efficiency to survey larger numbers.

A further caveat to note is that both Daddi et al. (2010) and Tacconi et al. (2010) apply corrections to their observed CO luminosities on account of the difference in the Rayleigh–Jeans brightness temperature of the higher J transitions targeted. Tacconi et al. (2010) apply $R_{31} = 0.5$ to their CO ($J = 3 \rightarrow 2$) luminosities (defined $R_{31} = L'_{\rm CO(3\rightarrow 2)}/L'_{\rm CO(1\rightarrow 0)}$), and Daddi et al. (2010) apply $R_{21} = 0.86$ to their CO ($J = 2 \rightarrow 1$) luminosities (see also Dannerbauer et al. 2009). Leroy et al. (2008) also apply $R_{21} = 0.8$ to a sub-sample of the $z \sim 0$ galaxies that were mapped in CO ($J = 2 \rightarrow 1$). Furthermore, Daddi et al. (2010) assume an $\alpha = 3.6 \pm 0.8$, inferred from dynamical mass arguments. Although this is within $\sim 1\sigma$ of the Galactic value, assuming $\alpha = 4.6$ increases the gas fraction by $\sim 12\%$. These systematic uncertainties in CO–H_2 conversions should be taken as a corollary when interpreting Figure 2, however, a large change in the gas mass (or stellar mass) would be required to remove the trend in $f_{\rm gas}$. It is unlikely that we have overestimated the gas mass in the $z = 0.4$ LIRGs, since we have applied $\alpha = 4.6$. In the high-z sources, the gas masses would have to be overestimated by a factor ~ 5, or the stellar masses underestimated by a factor ~ 4 to remove the trend.

5. SUMMARY

We have presented new constraints on the molecular gas mass of $z = 0.4$ LIRGs, showing strong evolution of $f_{\rm gas}$ since $z \sim 2$. The observed trend encodes critical information on the evolution of the growth of galaxies, including gas accretion, feedback, and stellar mass assembly. Future surveys that are able to split samples based on environment, mass, and other parameters will disentangle the relative effects that shape the evolution of the gas fraction. These observations will soon be supplemented and surpassed by progress made with the Atacama Large Millimeter Array and the Expanded Very Large Array, which will provide unprecedented sensitivity and resolution with which to probe the evolution of gas in galaxies.

This work was based on observations made with the IRAM PdBI, supported by INSU/CNRS (France), MPG (Germany), and IGN (Spain). We thank the anonymous referee for a constructive report. It is a pleasure to thank Roberto Neri for his support in this project. J.E.G. acknowledges the National Sciences and Engineering Research Council of Canada, support from the endowment of the Lorne Trottier Chair in Astrophysics and Cosmology (McGill) and the UK Science and Technology Facilities Council (STFC). I.R.S. and A.C.E. also acknowledge STFC.

REFERENCES

Blanton, M. R., & Roweis, S. 2007, AJ, 133, 734
Blitz, L., Fukui, Y., Kawamura, A., Leroy, A., Mizuno, N., & Rosolowsky, E. 2007, in Protostars and Planets V, ed. B. Reipurth, D. Jewitt, & K. Keil (Tucson, AZ: Univ. Arizona Press), 81
Blitz, L., & Rosolowsky, E. 2006, ApJ, 650, 933

Boissier, S., Prantzos, N., Boselli, A., & Gavazzi, G. 2003, MNRAS, 346, 1215
Coppin, K. E. K., et al. 2007, ApJ, 665, 936
Czoske, O., Kneib, J.-P., Soucail, G., Bridges, T. J., Mellier, Y., & Cuillandre, J.-C. 2001, A&A, 372, 391
Daddi, E., et al. 2008, ApJ, 673, L21
Daddi, E., et al. 2010, ApJ, 713, 686
Dannerbauer, H., Daddi, E., Riechers, D. A., Walter, F., Carilli, C. L., Dickinson, M., Elbaz, D., & Morrison, G. E. 2009, ApJ, 698, 178
Dutton, A. A., van den Bosch, F. C., & Dekel, A. 2010, MNRAS, 405, 1690
Elmegreen, B. G. 1993, ApJ, 338, 178
Fukugita, M., Hogan, C. J., & Peebles, P. J. E. 1998, ApJ, 503, 518
Geach, J. E., Smail, I., Coppin, K., Moran, S. M., Edge, A. C., & Ellis, R. S. 2009a, MNRAS, 395, L62 (G09)
Geach, J. E., Smail, I., Moran, S. M., Treu, T., & Ellis, R. S. 2009b, ApJ, 691, 783
Geach, J. E., et al. 2006, ApJ, 649, 661
Guilloteau, S., & Lucas, R. 2000, in ASP Conf. Ser. 217, Imaging at Radio Through Submillimeter Wavelengths, ed. J. G. Mangum & S. J. E. Radford (San Francisco, CA: ASP), 299
Harris, A. I., Baker, A. J., Zonak, S. G., Sharon, C. E., Genzel, R., Rauch, K., Watts, G., & Creager, R. 2010, ApJ, 723, 1139
Ivison, R. J., Papadopoulos, P. P., Smail, I., Greve, T. R., Thomson, A. P., Xilouris, E. M., & Chapman, S. C. 2011, MNRAS, tmp 46 (arXiv:1009.0749)
Karim, A., et al. 2010, arXiv:1011.6370
Kennicutt, R. C. 1998, ApJ, 498, 541
Kereš, D., Katz, N., Weinberg, D. H., & Davé, R. 2005, MNRAS, 363, 2
Komugi, S., Yasui, C., Kobayashi, N., Hatsukade, B., Kohno, K., Sofue, Y., & Kyu, S. 2010, PASJ, in press (arXiv:1011.3385)
Lagos, C., Lacey, C. G., Baugh, C. M., Bower, R. G., & Benson, A. J. 2010, arXiv:1011.5506
Leroy, A. K., Walter, F., Brinks, E., Bigiel, F., de Blok, W. J. G., Madore, B., & Thornley, M. D. 2008, AJ, 136, 2782
Moran, S. M., et al. 2007, ApJ, 671, 1503
Peng, C. Y., Ho, L. C., Impey, C. D., & Rix, H.-W. 2010, AJ, 139, 2097
Riechers, D. A., Carilli, C. L., Walter, F., & Momjian, E. 2010, ApJ, 724, L153
Solomon, P. M., Downes, D., Radford, S. J. E., & Barrett, J. W. 1997, ApJ, 478, 144
Tacconi, L. J., et al. 2010, Nature, 463, 781
Treu, T., Ellis, R. S., Kneib, J.-P., Dressler, A., Smail, I., Czoske, O., Oemler, A., & Natarajan, P. 2003, ApJ, 591, 53
Wong, T., & Blitz, L. 2002, ApJ, 569, 157